An Efficient Parallel FE-BI Algorithm for Large-scale Scattering Problems

Z. H. Fan, M. Chen, R. S. Chen, and D. Z. Ding

Department of Communication Engineering
Nanjing University of Science and Technology, China
Nanjing, P.R. China, 210094
eechenrs@mail.njust.edu.cn

Abstract ─In this paper, we present fast and accurate solutions of large-scale scattering problems involving three-dimensional objects with arbitrary shapes using parallel finite element-boundary integral method (FE-BI). Particularly, an efficient parallel preconditioner is constructed with both the finite-element matrix and the near-field part of the boundary integral equation operator for the ill-conditioned linear system formulated by the FE-BI. With an efficient parallelization of FE-BI, scattering problems that are discretized with millions of unknowns could be easily solved on distributed-memory computers. The numerical results are presented to demonstrate the accuracy and efficiency of the proposed method.

Index Terms **-** Finite element boundary integral method, parallelization, multilevel fast multipole method, scattering problems.

I. INTRODUCTION

The finite element boundary integral method (FE-BI) [1-5] provides fast and accurate solutions for three-dimensional electromagnetic scattering from complex geometries, which may be comprised of both conductors and dielectric media. The method divides the analyzed objects into two regions, one is the interior region and another is the exterior region. The field in the interior region is formulated using the finite-element method (FEM) and the field in the exterior region is represented by a boundary integral equation (BIE). The interior and exterior fields are then coupled by the field continuity conditions. In the FE-BI method, the final coefficient matrix is made up of a complex dense BIE sub-matrix and a complex sparse FEM sub-matrix. The multilevel fast multipole method (MLFMM) [6-10] is used to speed up the matrix-vector product (MVP) for the dense BIE part when the electrically large object is analyzed, which reduces the memory requirement from $O(N^2)$ to $O(NlogN)$ and the computational complexity from $O(N^3)$ to $O(NlogN)$, where N is the number of unknowns belongs to BIE part. When the FE-BI is combined with MLFMM, the coefficient matrix can be fast built when a large object is analyzed. Unfortunately, the FE-BI method suffers from a very slow convergence rate with the iterative solvers since the coefficient matrix arising from FE-BI is badly ill-conditioned. This bottleneck severely limits the capability of the FE-BI method since the iterative methods are the only choose for the large-scale problems. To break this bottleneck, many preconditioners have been developed to accelerate the convergence rate, such as the diagonal, block-diagonal, but they are not effective enough to yield a highly efficient solution. In [11], Liu and Jin proposed to use the FEM-absorbing boundary condition (ABC) matrix as the precondition for the FE-BI matrix equation. However, about 0.05 λ distance should be set between both the absorbing boundary and the scattering objects to improve the efficiency of the preconditioner. This will bring an increase of unknowns for the increscent calculation domain, which reduces the efficiency of the FE- ABC preconditioner. In this paper, an efficient preconditioner is constructed by the finite-element

Submitted On: March 6, 2011
Accepted On: September 12, 2011

part and the near-field value terms of the boundary integral, both can be easily obtained from the FE-BI matrix with no additional cost and memory requirement since the main contribution of the impedance matrix for the boundary integral is given by the near-field part. In our experience, the convergence rate of solving the FE-BI matrix is significantly accelerated after equipping this preconditioning technique.

Although the preconditioned FE-BI has been applied to a variety of electromagnetic problems with remarkable success, accurate solutions of many real-life problems require discretization with more than millions of unknowns, leading to large-scale matrix equations, which can not be solved on a single personal computer. In order to solve large problems, it is necessary to parallelize the FE-BI code and implement on distributed computers. However, it is not a trivial to design a high efficient parallelization scheme because of the complicated structure of the FE-BI matrices. Simple parallelization techniques usually fail to provide efficient solutions, due to communications among processors, poor loading-balance of the work. In this work, the FE-BI matrix is divided according to the features of the sub-matrices, which making it possible to compute and store only a small part of matrix in each computer and take full advantage of the parallelization computing. Especially, a series of implementation efforts previously developed for parallelizing the MLFMM in [12-19] are adopted to improve the parallelization efficiency of the BIE part, which is the most important point for the whole parallelization implementation. At the same time, the precondition matrix is constructed and factorized in parallelization.

The remainder of this paper is organized as follows. Section II gives a brief introduction to the FE-BI, together with an introduction of the novel preconditioner for the FE-BI. The parallization of FE-BI is also investigated in this part in detail. Section III presents the numerical results to demonstrate the accuracy and efficiency of the proposed method. Finally, some conclusions are given in section IV.

II. THEORY

Consider the problem of electromagnetic wave scattering by an inhomogeneous object characterized by relative permittivity ε_r and permeability μ_r . The object is excited by an incident field $\boldsymbol{E}^i(\boldsymbol{r})$ and the total field $\boldsymbol{E}(\boldsymbol{r})$ comprises the sum of the incident field $\boldsymbol{E}^i(\boldsymbol{r})$ and the scattered field $\boldsymbol{E}^s(\boldsymbol{r})$. To solve this problem with FE-BI, we first introduce a surface S to enclose the object and divide the object into an interior region and an exterior region. We employ the FEM to deal with the interior region. The exterior region is formulated using the BIE. The field inside S can be formulated into an equivalent variational problem with the functional given by

$$F(\mathbf{E})=\frac{1}{2jk_0}\iiint_V\left[\frac{1}{\mu_r}(\nabla\times\mathbf{E}(\mathbf{r}))\bullet(\nabla\times\mathbf{E}(\mathbf{r}))-k_0^2\varepsilon_r\mathbf{E}(\mathbf{r})\bullet\mathbf{E}(\mathbf{r})\right]dV+\eta_0\oiint_S(\mathbf{E}(\mathbf{r})\bullet\mathbf{J}_s(\mathbf{r}))dS, \quad (1)$$

where k_0 and η_0 denote the free-space wave number and impedance, respectively. V denotes the volume enclosed by S, $\hat{n}$ denotes the outward unit vector normal to S, K_0 is the free-space wave number. Using tetrahedron-based edge elements to expand $\mathbf{E}(\mathbf{r})$ and Rao-Wilton-Glisson (RWG) [20] basis functions to expand $\boldsymbol{J}_s$

$$\mathbf{E}=\sum_{i=1}^{M}E_i\mathbf{W}_i\ ,\quad \boldsymbol{J}_s=\sum_{i=1}^{N_s}J_i\mathbf{f}_i\ . \quad (2)$$

Substituting (2) into (1), we obtain the matrix equation

$$\begin{bmatrix}\boldsymbol{K}_{\mathrm{II}} & \boldsymbol{K}_{\mathrm{IS}} & 0\\ \boldsymbol{K}_{\mathrm{SI}} & \boldsymbol{K}_{\mathrm{SS}} & \boldsymbol{B}\end{bmatrix}\begin{Bmatrix}\boldsymbol{E}_{\mathrm{I}}\\ \boldsymbol{E}_{\mathrm{S}}\\ \boldsymbol{J}_{\mathrm{S}}\end{Bmatrix}=\begin{Bmatrix}0\\ 0\end{Bmatrix}, \quad (3)$$

where $\boldsymbol{E}_{\mathrm{I}}$ is a vector containing the discrete electric field inside V, $\boldsymbol{E}_{\mathrm{S}}$, and $\boldsymbol{J}_s$ are the vectors containing the discrete electric and magnetic field on S. $[\boldsymbol{K}_{\mathrm{II}}],[\boldsymbol{K}_{\mathrm{IS}}],[\boldsymbol{K}_{\mathrm{SI}}],[\boldsymbol{K}_{\mathrm{SS}}]$, and $[\boldsymbol{B}]$ denote the corresponding highly sparse FEM matrices, $[\boldsymbol{K}_{\mathrm{II}}]$ and $[\boldsymbol{K}_{\mathrm{SS}}]$ are symmetric matrices and $[\boldsymbol{K}_{\mathrm{IS}}]=[\boldsymbol{K}_{\mathrm{SI}}]^T$,where the superscript T denotes the transpose.

Equation (3) cannot be solved unless a relation between $\boldsymbol{E}_{\mathrm{S}}$ and $\boldsymbol{J}_s$ is established. Such a relation is provided by BIE for the exterior region, whose discretization yields

$$[\boldsymbol{P}]\{\boldsymbol{E}_{\mathrm{S}}\}+[\boldsymbol{Q}]\{\boldsymbol{J}_{\mathrm{S}}\}=\{\boldsymbol{b}\}\ . \quad (4)$$

In (4), $\{\boldsymbol{b}\}$ is a vector related to the incident

field. [$\boldsymbol{P}$] and [$\boldsymbol{Q}$] are generated by BIE. Combining (3) and (4) together, we obtain the following matrix equation

$$\begin{bmatrix} \boldsymbol{K}_{\mathrm{II}} & \boldsymbol{K}_{\mathrm{IS}} & 0 \\ \boldsymbol{K}_{\mathrm{SI}} & \boldsymbol{K}_{\mathrm{SS}} & \boldsymbol{B} \\ 0 & \boldsymbol{P} & \boldsymbol{Q} \end{bmatrix} \begin{Bmatrix} \boldsymbol{E}_{\mathrm{I}} \\ \boldsymbol{E}_{\mathrm{S}} \\ \boldsymbol{J}_{\mathrm{S}} \end{Bmatrix} = \begin{Bmatrix} 0 \\ 0 \\ \boldsymbol{b} \end{Bmatrix}. \quad (5)$$

The generation of (3) using FEM is standard, the generation of (4) using the method of moment (MoM) [20-21] can take many different forms. The basic equations for generating (4) are the electric-field integral equation (EFIE) is given by

$$\mathbf{E}^{inc}(\mathbf{r}) = \frac{1}{2}\mathbf{E}(\mathbf{r}) + \mathbf{L}(\bar{\mathbf{J}}_s) - \mathbf{K}(\mathbf{M}_s) \ , \quad (6)$$

and the magnetic-field integral equation (MFIE) is given by

$$\bar{\mathbf{H}}^{inc}(\mathbf{r}) = \frac{1}{2}\bar{\mathbf{H}}(\mathbf{r}) + \boldsymbol{L}(\mathbf{M}_s) + \boldsymbol{K}(\bar{\mathbf{J}}_s) \ , \quad (7)$$

where $\boldsymbol{J}$ and $\boldsymbol{M}$ are related to the fields on S by $\bar{\mathbf{J}}_s = \eta_0 \hat{n} \times \mathbf{H}$ and $\mathbf{M}_s = \mathbf{E} \times \hat{n}$, respectively, and ($\mathbf{E}^{inc}, \bar{\mathbf{H}}^{inc}$) denote the incident fields. The operators L and K are defined as

$$\mathbf{L}(\mathbf{X}) = jk_0 \iint_S \mathbf{X}(\mathbf{r}') G_0(\mathbf{r}, \mathbf{r}') \mathrm{d}S' + \iint_S \frac{j}{k_0} \nabla' \cdot \mathbf{X}(\mathbf{r}') \nabla G_0(\mathbf{r}, \mathbf{r}') \mathrm{d}S' \ , \quad (8)$$

$$\mathbf{K}(\mathbf{X}) = \iint_S \mathbf{X}(\mathbf{r}') \times \nabla G_0(\mathbf{r}, \mathbf{r}') \mathrm{d}S' \ . \quad (9)$$

However, each of them suffers from the problem of interior resonance and fails to produce accurate solutions at and near the resonant frequencies. To eliminate this problem, one has to combine EFIE and MFIE to obtain a combined field integral equation (CFIE). In this paper, the TE-NH is chosen which produces the best conditioned matrix for (5), substitute (2) into (6), we obtain the TE formulation

$$P_{mn} = \iint_S \mathbf{f}_m \cdot \left(-\frac{1}{2}\mathbf{w}_n(r) - \iint_S \mathbf{f}_n \times \nabla' G_0(\mathbf{r}, \mathbf{r}') \mathrm{d}S' \right) dS$$

$$= -\frac{1}{2} B_{mn} + \iint_S \mathbf{f}_m \cdot \iint_S \mathbf{f}_n \times \nabla G_0(\mathbf{r}, \mathbf{r}') \mathrm{d}S' dS \quad (10)$$

$$Q_{mn} = \iint_S \mathbf{f}_m \cdot \left(-jk_0 \iint_S \mathbf{f}_n G_0(\mathbf{r}, \mathbf{r}') \mathrm{d}S' - \iint_S \frac{j}{k_0} \nabla' \cdot \mathbf{f}_n(\mathbf{r}') \nabla G_0(\mathbf{r}, \mathbf{r}') \mathrm{d}S' \right) dS$$

$$= -jk_0 \iint_S \mathbf{f}_m \cdot \iint_S \mathbf{f}_n G_0(\mathbf{r}, \mathbf{r}') \mathrm{d}S' dS - \frac{1}{jk_0} \iint_S \nabla \cdot \mathbf{f}_m \iint_S \nabla' \cdot \mathbf{f}_n(\mathbf{r}') G_0(\mathbf{r}, \mathbf{r}') \mathrm{d}S' dS \ . \quad (11)$$

And from (7), the NH formulation

$$Q_{mn} = \left\langle \mathbf{f}_m, \frac{1}{2}\mathbf{f}_n(r) \right\rangle + \left\langle \mathbf{f}_m, \hat{n} \times \iint_S \mathbf{f}_n \times \nabla G_0(\mathbf{r}, \mathbf{r}') \mathrm{d}S' \right\rangle , \quad (12)$$

$$P_{mn} = -\hat{n} \times \mathbf{f}_m, jk_0 \iint_S \mathbf{f}_n G_0(\mathbf{r}, \mathbf{r}') \mathrm{d}S' - \iint_S \frac{j}{k_0} \nabla' \cdot \mathbf{f}_n(\mathbf{r}') \nabla G_0(\mathbf{r}, \mathbf{r}') \mathrm{d}S' \ . \quad (13)$$

The computational complexity of (5) consists of two parts: the part associated with FEM is $O(N)$ and the part related to BIE is $O(N_s^{\,2})$, where N_s denotes the number of unknowns on the truncation boundary. The dense matrices [$\boldsymbol{P}$] and [$\boldsymbol{Q}$] generated by the BIE are bottleneck of the FE-BI method, which severely limit the capacity of the FE-BI method in dealing with electrically large objects. Fortunately, this problem can be solved iteratively, where the required the MVP are performed efficiently by the MLFMM, which reduces the memory requirement and the computational complexity to $O(N_s \log N_s)$ for the BIE. Conventionally, to implement the MLFMM, an octree first needs to construct. The entire object is first enclosed in a large box, which is divided into eight smaller boxes. Each sub-box is then recursively subdivided into eight smaller cubes until the edge length of the finest cube is about half of a wavelength. The interaction between these boxes can be divided into two cases: two cubes are near each other sharing at least one edge point, the interaction between the two groups are computed by MoM. Otherwise, two cubes are well-separated from each other if the ratio of the cube-center-distance to the cube size is greater than or equal to 2. The interactions between boxes are calculated using the MLFMM.

The basic formulae to calculate the matrix entries for the far groups in MLFMM are given by

$$P_{ij} = (\frac{1}{2\lambda})^2 \int V_{im}^{P} T_{mm'}(\hat{k} \cdot \hat{r}_{mm'}) \cdot V_{jm'} d^2\hat{k} \ , \quad (14)$$

$$Q_{ij} = (\frac{1}{2\lambda})^2 \int V_{im}^{Q} T_{mm'}(\hat{k} \cdot \hat{r}_{mm'}) \cdot V_{jm'} d^2\hat{k} \ , \quad (15)$$

where

$$T_{mm'}(\hat{k} \cdot \hat{r}_{mm'}) = \sum_{l=0}^{L} (-j)^l (2l+1) h_l^{(2)}(k_0 r_{mm'}) \cdot P_l(\hat{r}_{mm'} \cdot \hat{k}) \ , \quad (16)$$

$$V_{im}^{P} = \int_S e^{-j\mathbf{k}_0 \cdot \mathbf{r}_{im}} [-\hat{k} \times \mathbf{f}_i + (\bar{\mathbf{I}} - \hat{k}\hat{k}) \cdot (\hat{n} \times \mathbf{f}_i)] dS \ , \quad (17)$$

$$V_{im}^{Q} = \int_S e^{-j\mathbf{k}_0 \cdot \mathbf{r}_{im}} \left[-\left(\bar{\mathbf{I}} - \hat{k}\hat{k} \right) \mathbf{f}_i - (\hat{k} \times \hat{n} \times \mathbf{f}_i) \right] dS \ , \quad (18)$$

$$V_{jm'} = \int_S e^{j\mathbf{k}_0 \cdot \mathbf{r}_{jm'}} \mathbf{f}_j dS \ . \quad (19)$$

Although the MLFMM for the BIE part has reduced the complexity of MoM from $O(N^2)$ to $O(N\log N)$, allowing the solution of large problems

with limited computational resources compared with the MoM. However, for problems with millions of unknowns, it is still not easy to solve it with FE-BI on a single processor. Thus, it is helpful to increase computational resource by assembling parallel computing platforms and, at the same time, by paralleling FE-BI.

A. Novel preconditioner in FE-BI

For equation (5), there are two approaches to solve it. One is the direct solver [22]; the other is the iterative solver. For large-scale problems, it is impractical to solve the matrix equation with a large number of unknowns using the direct solver. This difficulty can be circumvented by solving the matrix equation using the Krylov subspace iterative method, which requires the MVP in each iteration step. In the past, several iterative methods, including the conjugate gradient (CG), the biconjugate gradient (BCG), the stabilized biconjugate gradient (BCGS), and the generalized minimal residual (GMRES) have been employed. Unfortunately, since the BIE produces a dense matrix, the final FE-BI system matrix consists of a partly-full matrix and a partly-sparse matrix. The FE-BI matrix is usually ill-conditioned and requires a large number of iterations to reach convergence. Therefore for electrically large objects, iterative solvers should be adopted with efficient preconditioners. There are many preconditioners that have been developed to speed up the convergence rate of the GMRES solution, e.g. the block-diagonal can help to partially alleviate this difficulty, but they are not effective enough to yield a highly efficient solution. In [11], a FE-ABC preconditioner has been proposed and proven to be highly efficient for the FE-BI. However, a certain distance should be set between the absorbing boundary and the scattering objects to improve the efficiency of the preconditioner. This will bring the increase of the unknowns for the FE-BI. In this paper, an efficient preconditioner is constructed by the finite-element part and the near-field part of the boundary integral, both can be easily obtained from the matrix of the FE-BI with no additional computing cost and memory requirement since the main contribution of the impedance matrix for the boundary integral is given by the near-field part. Therefore, the preconditioning matrix is constructed by both the FEM matrix and the near-field part in the sparse pattern of the FEM matrix. Numerical results are presented to show the high effectiveness of the proposed method.

In this section, we consider solving the FE-BI matrix equation (5) with the MLFMM accelerated by the Krylov iterative method. In order to speed up the convergence rate of the Krylov iterative method, the preconditioning matrix $\boldsymbol{M}^{-1}$ is used to transform (5) into an equivalent form

$$\boldsymbol{M}^{-1}\boldsymbol{A}\boldsymbol{x} = \boldsymbol{M}^{-1}\boldsymbol{b}\,, \tag{20}$$

where

$$\boldsymbol{A} = \begin{bmatrix} \boldsymbol{K}_{\mathrm{II}} & \boldsymbol{K}_{\mathrm{IS}} & 0 \\ \boldsymbol{K}_{\mathrm{SI}} & \boldsymbol{K}_{\mathrm{SS}} & \boldsymbol{B} \\ 0 & \boldsymbol{P} & \boldsymbol{Q} \end{bmatrix} \quad \boldsymbol{x} = \begin{bmatrix} \boldsymbol{E}_{\mathrm{I}} \\ \boldsymbol{E}_{\mathrm{S}} \\ \boldsymbol{J}_{\mathrm{S}} \end{bmatrix} \quad \boldsymbol{b} = \begin{bmatrix} 0 \\ 0 \\ \boldsymbol{b} \end{bmatrix}.$$

With $\tilde{\boldsymbol{A}} = \boldsymbol{M}^{-1}\boldsymbol{A}$ and $\tilde{\boldsymbol{b}} = \boldsymbol{M}^{-1}\boldsymbol{b}$, equation (20) can be written as the following form

$$\tilde{\boldsymbol{A}}\boldsymbol{x} = \tilde{\boldsymbol{b}}\,. \tag{21}$$

$\boldsymbol{M}^{-1}$ is a matrix for preconditioning the matrix $\boldsymbol{A}$ from the left. The purpose of preconditioning is to make the condition number of the matrix $\tilde{\boldsymbol{A}}$ better than the original matrix $\boldsymbol{A}$. Thus, the Krylov iterative method for the equation (21) can get a fast convergence.

An effective preconditioner $\boldsymbol{M}$ [22-23] should be a good approximation of matrix $\boldsymbol{A}$ and easy to construct. Since the main contribution of the impedance matrix for the boundary integral is given by the near-field part. The preconditioner is constructed by the finite-element part and the near-field of the BIE matrix in sparse pattern as shown in (22); both can be easily obtained from the FE-BI matrix with no additional computing cost and memory requirement.

$$\boldsymbol{M} = \begin{bmatrix} \boldsymbol{K}_{\mathrm{II}} & \boldsymbol{K}_{\mathrm{IS}} & 0 \\ \boldsymbol{K}_{\mathrm{SI}} & \boldsymbol{K}_{\mathrm{SS}} & \boldsymbol{B} \\ 0 & \boldsymbol{P}' & \boldsymbol{Q}' \end{bmatrix}. \tag{22}$$

Then (20) can be written as follows

$$\begin{bmatrix} \boldsymbol{K}_{\mathrm{II}} & \boldsymbol{K}_{\mathrm{IS}} & 0 \\ \boldsymbol{K}_{\mathrm{SI}} & \boldsymbol{K}_{\mathrm{SS}} & \boldsymbol{B} \\ 0 & \boldsymbol{P}' & \boldsymbol{Q}' \end{bmatrix}^{-1} \begin{bmatrix} \boldsymbol{K}_{\mathrm{II}} & \boldsymbol{K}_{\mathrm{IS}} & 0 \\ \boldsymbol{K}_{\mathrm{SI}} & \boldsymbol{K}_{\mathrm{SS}} & \boldsymbol{B} \\ 0 & \boldsymbol{P} & \boldsymbol{Q} \end{bmatrix} \begin{Bmatrix} \boldsymbol{E}_I \\ \boldsymbol{E}_S \\ \boldsymbol{J}_S \end{Bmatrix} = \begin{bmatrix} \boldsymbol{K}_{\mathrm{II}} & \boldsymbol{K}_{\mathrm{IS}} & 0 \\ \boldsymbol{K}_{\mathrm{SI}} & \boldsymbol{K}_{\mathrm{SS}} & \boldsymbol{B} \\ 0 & \boldsymbol{P}' & \boldsymbol{Q}' \end{bmatrix}^{-1} \begin{Bmatrix} 0 \\ 0 \\ \boldsymbol{b} \end{Bmatrix}. \tag{23}$$

In order to reduce the computational complexity of the MVP, the second matrix in the left terms of (23) can be replaced according to the following

equation

$$\begin{bmatrix} \boldsymbol{K}_{\mathrm{II}} & \boldsymbol{K}_{\mathrm{IS}} & 0 \\ \boldsymbol{K}_{\mathrm{SI}} & \boldsymbol{K}_{\mathrm{SS}} & \boldsymbol{B} \\ 0 & \boldsymbol{P} & \boldsymbol{Q} \end{bmatrix} = \begin{bmatrix} \boldsymbol{K}_{\mathrm{II}} & \boldsymbol{K}_{\mathrm{IS}} & 0 \\ \boldsymbol{K}_{\mathrm{SI}} & \boldsymbol{K}_{\mathrm{SS}} & \boldsymbol{B} \\ 0 & \boldsymbol{P}' & \boldsymbol{Q}' \end{bmatrix} - \begin{bmatrix} 0 & 0 & 0 \\ 0 & 0 & 0 \\ 0 & \boldsymbol{P}-\boldsymbol{P}' & \boldsymbol{Q}-\boldsymbol{Q}' \end{bmatrix}, \quad (24)$$

and (24) can be sequentially transformed to the following form

$$\left\{ \boldsymbol{I} + \begin{bmatrix} \boldsymbol{K}_{\mathrm{II}} & \boldsymbol{K}_{\mathrm{IS}} & 0 \\ \boldsymbol{K}_{\mathrm{SI}} & \boldsymbol{K}_{\mathrm{SS}} & \boldsymbol{B} \\ 0 & \boldsymbol{P}' & \boldsymbol{Q}' \end{bmatrix}^{-1} \begin{bmatrix} 0 & 0 & 0 \\ 0 & 0 & 0 \\ 0 & \boldsymbol{P}-\boldsymbol{P}' & \boldsymbol{Q}-\boldsymbol{Q}' \end{bmatrix} \right\} = \begin{bmatrix} \boldsymbol{K}_{\mathrm{II}} & \boldsymbol{K}_{\mathrm{IS}} & 0 \\ \boldsymbol{K}_{\mathrm{SI}} & \boldsymbol{K}_{\mathrm{SS}} & B \\ 0 & \boldsymbol{P}' & \boldsymbol{Q}' \end{bmatrix}^{-1} \begin{Bmatrix} 0 \\ 0 \\ \boldsymbol{b} \end{Bmatrix}, \quad (25)$$

where $\boldsymbol{P}'$ and $\boldsymbol{Q}'$ stand for the near-field part drawing from the total matrix of boundary integral $\boldsymbol{P}$ and $\boldsymbol{Q}$ in the sparse pattern of FEM matrices $\boldsymbol{B}$ and $\boldsymbol{K}_{SS}$, respectively.

For sequential implementations of the FE-BI running on a single processor, the calculation of $\boldsymbol{M}^{-1}$ can be obtained by the UMFPACK strategy [24]. However, for large-scale problems, the direct solver $\boldsymbol{M}^{-1}$ may require prohibitive memory and the time used to construct the matrix $\boldsymbol{M}^{-1}$ will be very long. Fortunately this cost can be alleviated by parallelization. In this paper, we use the parallel LU factorization to construct the preconditioner matrix $\boldsymbol{M}^{-1}$, after decomposing the matrix $\boldsymbol{M}$ in the form of $\boldsymbol{M} = \boldsymbol{L}\bullet\boldsymbol{U}$. The preconditioning operation is performed in each step by solving $\boldsymbol{L}\bullet\boldsymbol{U}\bullet\boldsymbol{v} = \boldsymbol{w}$, the preconditioning operation $\boldsymbol{v} = \boldsymbol{M}^{-1}\boldsymbol{w}$ is computed by solving the linear system $\boldsymbol{L}\bullet\boldsymbol{U}\bullet\boldsymbol{v} = \boldsymbol{w}$, it is performed at two distinct steps: solve $\boldsymbol{L}\boldsymbol{x} = \boldsymbol{w}$ and $\boldsymbol{U}\boldsymbol{v} = \boldsymbol{x}$ successively. This two-step is processing in parallization. We call this preconditioning iteration as a forward and backward preconditioning iteration.

B. Efficient parallelization of FE-BI matrix

Because of the complicated structure of the FE-BI matrix, parallelization of FE-BI is not trivial. Simple parallelization schemes usually lead to inefficient solutions due to dense communications and unbalanced distribution of the workload among processors. For high efficiency parallelization, two parts must be considered in detail. The first part is to partition the MoM matrices among the distribute computers. The second part is to construct the preconditioner matrices among the distribute computers. For the FEM matrix $[\boldsymbol{K}_{\mathrm{II}}]$, $[\boldsymbol{K}_{\mathrm{IS}}]$, $[\boldsymbol{K}_{\mathrm{SI}}]$, $[\boldsymbol{K}_{\mathrm{SS}}]$, and $[\boldsymbol{B}]$, which denotes the corresponding highly sparse FEM matrix. This estimation needs very small memory and CPU time; thus, all the FEM matrices are computed on one processor.

For the surface MoM matrices generated by the BIE are a bottleneck of the FE-BI, which severely limits the capacity of the FE-BI method in dealing with electrically large objects. Although the MLFMM allows for it to solve large problems with limited computational resources, to further improve the capacity of the MLFMM for electrically large objects, one of robust ways is to increase computational resources by assembling parallel computer platforms and, at the same time, by parallelizing MLFMM.

The efficiency of the parallel FE-BI is determined by the efficiency of the parallel BIE part. In the past few years, a series of implementation tricks have been developed for efficiently parallelizing the MLFMM, these tricks are different, but the key issues in those tricks in parallelizing MLFMM are load-balancing and minimizing the communications between the processors. To obtain an efficient parallelization of MLFMM, several issues must be carefully considered to distribute the task equally among the processors. In this paper, we utilize different partitioning strategies for the lower and higher levels of the tree structure. It is natural that the parallel approach for the fine level is to distribute the boxes equally among processors, where the number of boxes is much larger than the number of processors. But it is difficult to achieve good load-balancing for the coarse level with this parallel approach, where the number of boxes is smaller than the number of processors. However, since the box size of the coarse level is big, and the number of far-field patterns for the MLFMM is large, we can partition the far-field patterns equally among all processors while replicating the boxes in every processor as paper [16]. Using this scheme for the parallel MLFMM in the far-field, good load balancing can be achieved.

The interaction matrix in MLFMM is classified

into a near-field interaction matrix and a far-field interaction matrix. After distributing the boxes to each processor in the finest level, the near-field and the far-field interaction lists can be set up in a parallel way. The near-field interaction matrix are calculated directly and stored in memory. For the far-field, the interaction is calculated in a cluster-by-cluster manner. The computation in MLFMM is done in three stages called the aggregation, translation and disaggregation stage.

Aggregation stage: The far-field interaction begins with aggregating basis functions at the finest level to obtain the radiation pattern. Each processor calculates and stores the radiation and receiving patterns of the basis and testing functions included in its local box. Then each processor shifting the radiation pattern to the center of the box in the second finest level, and finally interpolating the deficient radiation pattern to obtain the radiation pattern of the box in the second-finest level. This procedure repeats until the shared levels. In the shared levels, each box is assigned to the same processor. The far-field pattern of each box is distributed equally among processors. In the distributed levels, even though a local interpolation is used, some of the far-field patterns may locate in other processors. Therefore one-to-one communications are needed to get the required data.

Translation stage: The translation stage is one of the most important stages in the parallelization MLFMM; since the boxes are distributed among the processors; one to one communications are required between the processors for the translation stage. To eliminate this overhead, each processor is loaded with extra boxes called the ghost boxes. For example, if box i at processor a needed the far-field samples of box j at processor b, maybe another box at processor a also needed the far-field samples of box j, to reduce the communication between the processors; we allocate space for the box j at processor a. When the far-field samples of box j is received by processor a, we store it in the memory, this ensure that the same data is not transferred more than once. In the shared levels, the far-field samples of each cluster are distributed equally among the processors. Therefore, there is no need for communication between the processors at the translation stage in the shared levels.

Disaggregation stage: The disaggregation stage is the generally the inverse of the aggregation stage, the incoming fields are calculated at the centre of each box from the top of the tree structure to the lowest level using the anterpolation. Some of the far-field samples obtained from the anterpolation operation should be sent to other processors in the distributed levels, Similar to the communications during the aggregation stage, this procedure repeats until the finest level.

III. NUMERICAL RESULTS

In this section, several numerical examples are presented to demonstrate the efficiency of the proposed method. All experiments are performed on two distributed-memory computers; each computer involves 8 processors, each processor has 6 gigabytes (GB) of memory with 3.0GHz clock rate. The resulting linear systems are solved iteratively by the GMRES (30) solver with a relative residual of 10^{-3} in double precision.

A. The accuracy of the proposed method

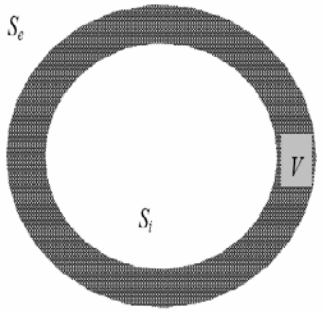

Fig. 1. A PEC sphere coated with a single-layer dielectric.

First, the proposed method is used to analyze scattering from a perfect conductor (PEC) sphere having a diameter of 16λ, the sphere is coated with a 0.1m thick dielectric layer having a relative permittivity of $\varepsilon_r = 2 - i$ and $\mu_r = 1$ as shown in Fig. 1, S_i is the surface of the PEC sphere. A 400MHz plane wave is incident at $\theta_{inc} = 0$, $\phi_{inc} = 0$ and the observed scattering angles are $\theta_s = 0 \sim 180^\circ$ at $\phi_s = 0^\circ$. During the FE-BI calculation for this example, the boundary integral is carried out on the outer surface of the dielectric sphere. The total number of unknowns is 3,540,000, consisting of

2,710,000 for the finite-element and 830,000 for the boundary integral. We first assume that the sphere coated with an air, thus, the bistatic radar cross section (RCS) of the coated sphere is equal to a PEC sphere. As shown in Fig. 2, the numerical result of the bistatic RCS of the sphere is in a good agreement with the Mie solution. Figure 3 shows the bistatic RCS of the sphere coated with dielectric, the dielectric is characterized by $\varepsilon_r = 2 - i$ and $\mu_r = 1$. It can also be found that there is a good agreement with the Mie solution. It involves 52 iterations for this problem to reach convergence.

Solutions are performed on 1, 4, 8, 16, and 32 processors, respectively. Table I lists the total processing times including the setup time and iterative solution parts, and the parallelization efficiency obtained for 4, 8, 16, and 32 processors with respect to 1 processor. Ideally, the speed of a simulation with P processors is P times higher compared with a single processor and the efficiency is 100%. However, from Table I we can see that when the number of processors increases, the efficiency of the FE-BI decreases. This is because with the number of processors increases, although the time for matrix computing decreases correspondingly, the data communication time in the translation stage between the computer increases quickly when the number of processors increases. This becomes the bottleneck in the parallelization of FE-BI.

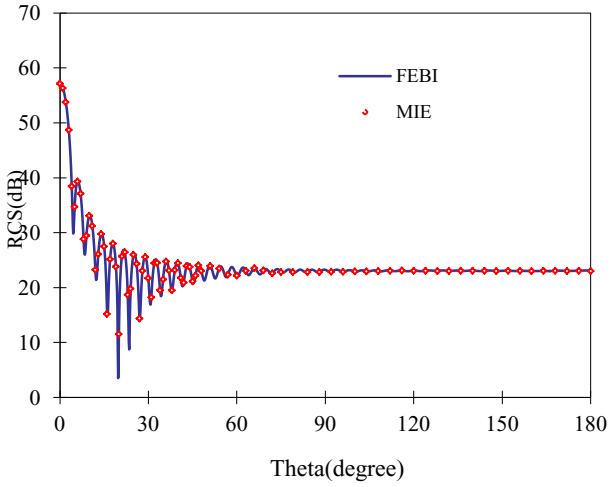

Fig. 2. Bistatic RCS of the conduct sphere at 400 MHz.

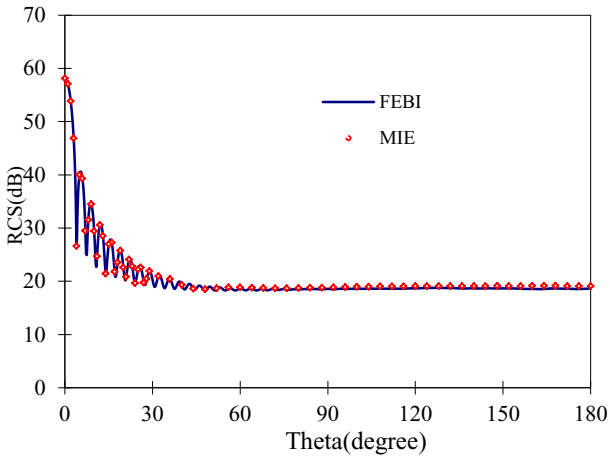

Fig. 3. Bistatic RCS of the coated sphere at 400 MHz.

Table I: Total processing time and parallelization for the solution of the sphere discretized with 3,540,000 unknowns

Sphere (Radius:16 λ , Number of unknowns: 3,540,000)					
Number of Processors	1	4	8	16	32
Total time (mintues)	219	58	33	18	11
Efficiency	100%	94%	83%	76%	62%

The second geometry is a coated cylinder with a diameter of 10 λ and 20 λ high, the cylinder is coated with 0.1m thick dielectric layer having a relative permittivity of $\varepsilon_r = 2 - i$ and $\mu_r = 1$. A 500MHz plane wave is incident at $\theta_{inc} = 0$ and $\phi_{inc} = 0$, and the observed scattering angles are $\theta_s = 0 \sim 180$ at $\phi_s = 0$. After discretisation, the number of unknowns is 3,100,000, consisting of 2,260,000 for the finite-element, and 840,000 for the boundary integral. We first consider the cylinder coated with air, so the RCS of the coated cylinder is equal to a PEC cylinder, Fig. 5 shows the bistatic RCS of the cylinder coated with dielectric $\varepsilon_r = 2 - i$ and $\mu_r = 1$. The numerical results of the bistatic RCS are compared with the body of revolution (BOR). It can be seen from Fig. 4 and Fig. 5 that there is a good agreement between the parallel FE-BI and BOR. It involves 44 iterations for this problem to reach convergence. Table II lists the total processing times including the setup time and iterative solution parts, and the parallelization efficiency obtained for 4, 8, 16, and 32 processors with respect to 1 processor. From the two examples

above, we can see that the parallelization of the FE-BI provides an efficient approach to solve large-scale electromagnetic scattering problems.

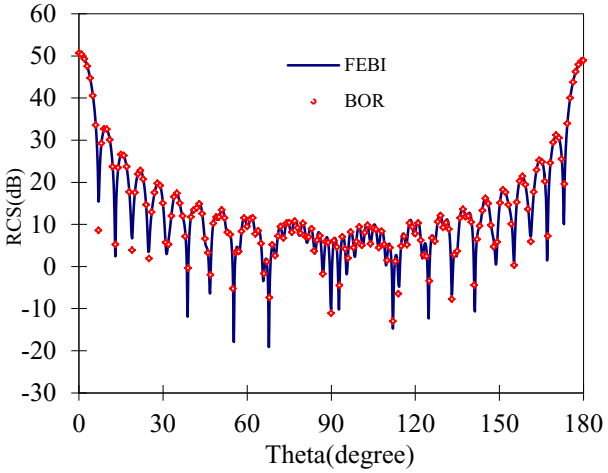

Fig. 4. Bistatic RCS of the PEC cylinder at 500 MHz.

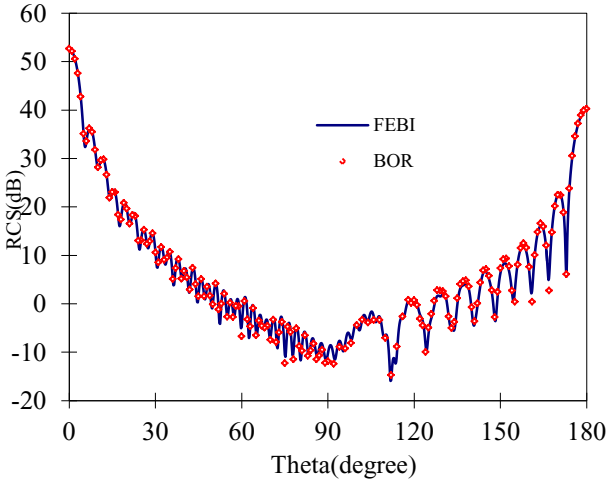

Fig. 5. Bistatic RCS of the coated cylinder at 500 MHz.

Table II: Total processing time and parallelization for the solution of the cylinder discretized with 3,100,000 unknowns

Cylinder (Diameter of 10 λ and 20 λ high , Number of unknowns: 3,100,000)					
Number of Processors	1	4	8	16	32
Total time (mintues)	171	45	26	14	9
Efficiency	100%	95%	82%	76%	59%

B. Solution of the real-life problem

To further show the capacity of our parallel FE-BI code, finally, we present the solutions of a real-life problem involving an airplane as shown in Fig. 6. The airplane is coated with a 0.02 wavelength thick dielectric layer having a relative permittivity of $\varepsilon_r = 4$ and $\mu_r = 2 - i$. A 600MHz plane wave is incident at $\theta_{inc} = 120^\circ$, $\phi_{inc} = 270^\circ$ and the observed scattering angles are $\theta_s = 120^\circ$ at $\phi_s = 0 \sim 360^\circ$. The bistatic RCS of the coated airplane is presented in Fig. 6. After the setup, it takes about 24 minutes, and the iterative solution involves 49 iterations to solve the problem on 16 processors.

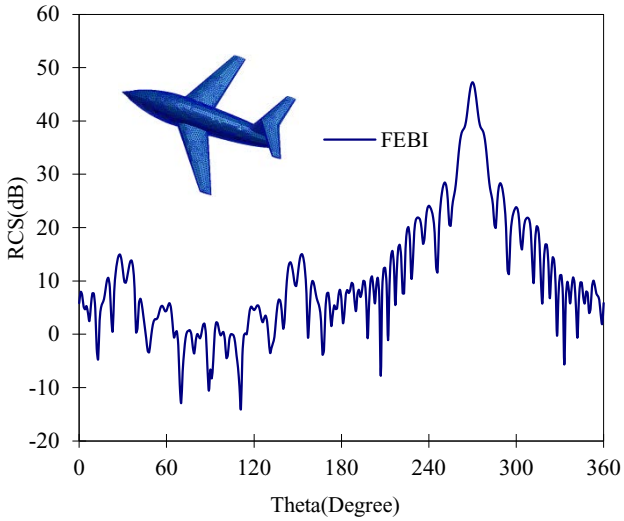

Fig. 6. Bistatic RCS of the coated airplane at 600 MHz.

IV. CONCLUSIONS

In this paper, we consider fast and accurate solutions of large-scale scattering problems discretized with millions of unknowns using a parallel FE-BI on distributed-memory computers. The parallel near-field preconditioner is used to accelerate the convergence speed of the FE-BI matrix iteration. The capacity of the parallel FE-BI has been demonstrated by computing several coated geometries, i.e. a sphere, a cylinder, and an airplane. From the numerical results, we can see that the proposed parallel FE-BI is efficient for solving the scattering of electrically large objects.

REFERENCES

[1] M. M. Botha and J. M. Jin, "On the Variational Formulation of Hybrid Finite Element-Boundary Integral Techniques for Electromagnetic Analysis," *IEEE Trans. Antennas and Propag.,* vol. 52, no. 11, pp. 3037-3047, November 2004.

[2] C. Guo and T. H. Hubing, "Development and Application of a Fast Multipole Method in a Hybrid FEM/MoM Field Solver," *Applied Computational Electromagnetic Society (ACES) Journal,* vol. 19, no. 3, pp. 126-134, November 2004.

[3] X. Q. Sheng, J. M. Jin, J. M. Song, C. C. Lu, and W. C. Chew, "On the Formulation of Hybrid Finite-Element and Boundary-Integral Methods for 3D Scattering using Multi-Level Fast Multipole Algorithm," *IEEE Antennas and Propagation Society International Symposium.,* pp. 236 – 239, vol. 1,1998.

[4] X. Q. Sheng, J. M. Jin, J. M. Song, C. C. Lu, and W. C. Chew, "On the Formulation of Hybrid Finite-Element and Boundary-Integral Methods for 3-D Scattering," *IEEE Trans. Antennas and Propag.,* vol. 46, no. 3, pp. 303 – 311, March 1998.

[5] P. Demarcke and H. Rogier, "Hybrid Finite Element-Boundary Integral Method Accelerated by the NSPW-MLFMA," *Electromagnetic Theory (EMTS),* 2010 URSI International Symposium on, pp. 463 - 466, 2010.

[6] H. Chen, Z. H. Fan, R. S. Chen, Z. N. Jiang, and M. M. Li, "Adaptive Mixed-Form Fast Multipole Method for the Analysis of Electromagnetic Scattering," *Applied Computational Electromagnetic Society (ACES) Journal,* vol. 25, no. 11, November 2010.

[7] R. Coifman, V. Rokhlin, and S. M. Wandzura, "The Fast Multipole Method for the Wave Equation: A Pedestrian Prescription," *IEEE Trans. Antennas and Propag.,* vol. 35, no. 3, pp. 7-12, June. 1993.

[8] J. M. Song, C. C. Lu, and W. C. Chew, "Multilevel fast multipole algorithm for Electromagnetic scattering by large complex objects," *IEEE Trans. Antennas and Propag.,* vol. 45, no.10, pp. 1488-1493, October 1997.

[9] C. C. Lu and W. C. Chew, "A Multilevel Algorithm for Solving Boundary Integral Equations of Wave Scattering," *Micro. Opt. Tech. Lett.,* vol. 7, pp. 466-470, July 1994.

[10] J. M. Song and W. C. Chew, "Multilevel Fast-Multipole Algorithm for Solving Combined Field Integral Equation of Electromagnetic Scattering," *Micro. Opt. Tech. Lett.,* vol. 10, pp. 14-19, Sept. 1995.

[11] J. Liu and J.-M. Jin, "A Highly Effective Preconditioner for Solving the Finite Element Boundary Integral Matrix Equation of 3-D Scattering," *IEEE Trans. Antennas and Propag.,* vol. 50, no. 9, pp. 1212-1221, September 2002.

[12] H. Zhao, J. Hu, and Z. Nie, "Parallelization of MLFMA with Composite Load Partition Criteria and Asynchronous Communication," *Applied Computational Electromagnetic Society (ACES) Journal,* vol. 25, no. 2, pp. 167-173, February 2010.

[13] H. Fangjing, N. Zaiping, and H. Jun, "An Efficient Parallel Multilevel Fast Multipole Algorithm for Large-scale Scattering Problems," *Applied Computational Electromagnetic Society (ACES) Journal,* vol. 25, no. 4, pp. 381-387, April 2010.

[14] K. C. Donepudi and J. M. Jin et al, "A higher Order Parallelized Multilevel Fast Multipole Algorithm for 3-D Scattering," *IEEE Trans. Antennas and Propag.,* vol. 49, no. 7, pp. 1069-1078, July 2001.

[15] W. Rankin and J. Board, "A Potable Distributed Implementation of the Parallel Multipole Tree Algorithm." *Proceedings of IEEE Symposimu on High Performance Distributed Computing.,* pp. 17-22,1995.

[16] X. M. Pan and X. Q. Sheng, "A Sophisticated Parallel MLFMM for Scattering by Extremely Large Targets," *IEEE Trans. Antennas and Propag.,* vol. 50, no. 3, pp. 129-138, June 2008.

[17] O. Ergul and L. Gurel, "Efficient Parallelization of the Multilevel Fast Multipole Algorithm for the Solution of Large-Scale Scattering Problems," *IEEE Trans. Antennas and Propag.,* vol. 56, no. 8, pp. 2335-2345, August 2008.

[18] O. Ergul and L. Gurel, "A Hierarchical Partitioning Strategy for an Efficient Parallelization of the Multilevel Fast Multipole Algorithm," *IEEE Trans. Antennas and Propag.,* vol. 57, no. 6, pp. 1740-1750, June 2009.

[19] J. Fostier and F. Olyslager, "An Asynchronous Parallel MLFMA for Scattering at Multiple Dielectric Objects," *IEEE Trans. Antennas and Propag.,* vol. 56, no. 8, pp. 2346-2355, August 2008.

[20] S. M. Rao, D. R. Wilton, and A. W. Glisson, "Electromagnetic Scattering by Surfaces of Arbitrary Shape," *IEEE Trans. Antennas and Propag.,* vol. 30, no. 3, pp. 409-418, 1982.

[21] B. J. Fasenfest, F. Capolino, and D. R. Wilton, "Preconditioned GIFFT: A Fast MoM Solver for Large Arrays of Printed Antennas," *Applied Computational Electromagnetic Society* (*ACES) Journal,* vol. 21, no. 3, pp. 276-283, November 2006.

[22] Z. N. Jiang, Z. H. Fan, D. Z. Ding, R. S. Chen, and K. W. Leung, "Preconditioned MDA-SVD-MLFMA for Analysis of Multi-scale Problems,"

Applied Computational Electromagnetic Society (ACES) Journal, vol. 25, no. 11, November 2010.

[23] P. L. Rui, R. S. Chen, D. X. Wang, E. K. N. Yung, "A Spectral Multigrid Method Cobined with MLFMM for Solving Elelctromegnetic Wave Scattering Problems," *IEEE Trans. Antennas and Propag.,* vol. 55, no. 9, pp. 1-7, September 2007.

[24] T. A. Davis "Algorithm 832: UMFPACK, an Unsymmetric-Pattern Multifrontal Method," *ACM Trans. Math.Softw.*, 30, pp. 196-199, 2003.

Zhen-Hong Fan was born in Jiangsu, the People's Republic of China in 1978. He received the M.Sc. and Ph.D. degrees in Electromagnetic Field and Microwave Technique from Nanjing University of Science and Technology (NJUST), Nanjing, China, in 2003 and 2007, respectively. During 2006, he was with the Center of Wireless Communication in the City University of Hong Kong, Kowloon, as a Research Assistant. He is currently an associated Professor with the Electronic Engineering of NJUST. He is the author or coauthor of over 20 technical papers. His current research interests include computational electromagnetics, electromagnetic scattering and radiation.

Ming Chen was born in Anhui, China. He received the B.S. degree in Physics from Anhui University in 2006, and is currently working toward the Ph.D. degree at Nanjing University of Science and Technology (NJUST), Nanjing, China. His current research interests include computational electromagnetics, antennas, and electromagnetic scattering and propagation.

Ru-Shan Chen was born in Jiangsu, P. R. China. He received his B.Sc. and M.Sc. degrees from the Dept. of Radio Engineering, Southeast University, in 1987 and in 1990, respectively, and his Ph.D. from the Dept. of Electronic Engineering, City University of Hong Kong in 2001. He became a Teaching Assistant in 1990 and a Lecturer in 1992. Since September 1996, he has been a Visiting Scholar with the Department of Electronic Engineering, City University of Hong Kong, first as Research Associate, then as a Senior Research Associate in July 1997, a Research Fellow in April 1998, and a Senior Research Fellow in 1999. From June to September 1999, he was also a Visiting Scholar at Montreal University, Canada. In September 1999, he was promoted to Full Professor and Associate Director of the Microwave & Communication Research Center and in 2007, he was appointed Head of the Dept of Communication Engineering, Nanjing University of Science & Technology (NJUST). His research interests mainly include microwave/millimeter-wave systems, measurements, antenna, RF-integrated circuits, and computational electromagnetics. He is a Senior Member of the Chinese Institute of Electronics (CIE). He received the 1992 third-class science and technology advance prize given by the National Military Industry Department of China, the 1993 third class science and technology advance prize given by the National Education Committee of China, the 1996 second-class science and technology advance prize given by the National Education Committee of China, and the 1999 first-class science and technology advance prize given by JiangSu Province as well as the 2001 second-class science and technology advance prize. At NUST, he was awarded the Excellent Honor Prize for academic achievement in 1994, 1996, 1997, 1999, 2000, 2001, 2002, and 2003. He has authored or co-authored more than 200 papers, including over 140 papers in international journals. He is the recipient of the Foundation for China Distinguished Young Investigators presented by the National Science Foundation (NSF) of China in 2003. In 2008, he became a Chang-Jiang Professor under the Cheung Kong Scholar Program awarded by the Ministry of Education, China.

Dazhi Ding was born in Jiangsu, the People's Republic of China. He received the B.S. and Ph.D. degrees in Electromagnetic Field and Microwave Technique from Nanjing University of Science and Technology (NJUST), Nanjing, China, in 2002 and 2007, respectively. During 2005, he was with the Center of Wireless Communication in the City University of Hong Kong, Kowloon, as a Research Assistant. He is currently a Lecturer with the Electronic Engineering of NJUST. He is the author or coauthor of over 20 technical papers. His current research interests include computational electromagnetics, electromagnetic scattering and radiation.